Published in IET Microwaves, Antennas & Propagation
Received on 21st December 2011
Revised on 24th May 2012
doi: 10.1049/iet-map.2011.0606

ISSN 1751-8725

Four-port beam reconfigurable antenna array for pattern diversity system

V.-A. Nguyen M.-H. Jeong M.-T. Dao S.-O. Park

Microwave and Antenna Lab, Korean Advanced Institute of Science and Technology
E-mail: ngvanh78@yahoo.com

Abstract: This study investigates a practical design for a switched beam planar antenna that can be implemented as a compact, low-cost switchable and/or reconfigurable beam antenna array. The antenna consists of a four-port antenna array, which is based on L-shaped quarter-wavelength slot antenna elements. This type of antenna array is a planar structure and its maximum directional radiation beam pattern presents in an azimuth plane covering 360°. The antenna array operates based on the 'ON' or 'OFF' states of PIN diodes in each individual slot antenna element and the combined signals from the four-port output. Therefore by properly controlling the state of the PIN diodes, the antenna exposes its characteristics of switchable/reconfigurable beam patterns in the Φ-plane. To validate the proposed design, a small smart, switched-beam antenna operating at 2.7 GHz in multiple input-multiple output applications is simulated and fabricated.

1 Introduction

In recent years, reconfigurable antennas have received significant attention in the field of wireless communications [1]. These antennas are capable of achieving selectivities in the operating frequencies, polarisations, radiation patterns, as well as gains. In modern wireless systems, data streams always propagate in a multipath environment and encounter sever interference from reflections or diffraction from buildings, landforms or near-by objects. In addition, systems operated in adjacent frequency channels may also give rise to significant performance degradation. To resolve these problems, several techniques are commonly used to increase the signal-to-noise ratio and the overall performance such as diversity techniques (spatial diversity, pattern diversity, temporal diversity and polarisation diversity), and multiple input-multiple output (MIMO). Diversity capability can be achieved in a straightforward manner by using a reconfigurable antenna with the beam pattern alternatively switched between several predetermined directions as presented in [1–16]. MIMO systems can improve wireless performance without increasing transmitting power and/or radio spectrum [3, 6, 7, 11]. However, the advantages of the aforementioned methods come at the expense of (i) increased size of configuration; (ii) increased significant complexity in the baseband processing; and (iii) the need for multiple radiofrequency (RF) front-ends.

Alternatively, compact and simplified smart antennas can provide performance enhancement with less complexity and lower cost. One of the approaches to simplify the design of smart antennas is to use an antenna array for which the beam patterns can be electronically selected by digital baseband signals. By properly selecting the available beam patterns to fit the direction of the desired incoming signal, we can minimise affects from interfering signals, and thus the wireless performance is much improved. Various attempts have been made to simplify smart antennas, including smart antenna arrays and adaptive antenna arrays [12–16]. These approaches use expensive components with intricate circuits that may lead to higher cost systems.

Within the scope of this work, we propose and validate the design of a switched-beam planar antenna. The proposed design can be implemented as a compact and low-cost switchable and/or reconfigurable beam antenna array without a phase shifter network. In Section 2.1, we present the details of the proposed antenna, which is composed of four equal ports and eight L-shaped slots etched on all four corners of the middle ground layer. In Sections 2.2 and 2.3, we validate the new concept by designing and implementing a 2.6–2.8-GHz switched beam antenna for small smart antenna applications. Sections 3 and 4 describe the simulation and measurement of a prototype.

2 Proposed antenna array design

2.1 Antenna element and array configuration

The structure and notation of the proposed antenna array are described in Fig. 1*a*. We use two printed circuit board layers of FR4 substrate sharing a common ground in the middle (condition 2). The top metal layer (condition 1) contains the microstrip feed line, whereas the bottom metal layer (condition 3) contains the bias network (as in Fig. 1). The details of the planar slot-type antenna structure and its dimension are shown in Fig. 1*d* and Table 1, respectively. The characteristic and the radiation property of the conventional L-shaped quarter-wavelength slot antenna are presented in [4–9].

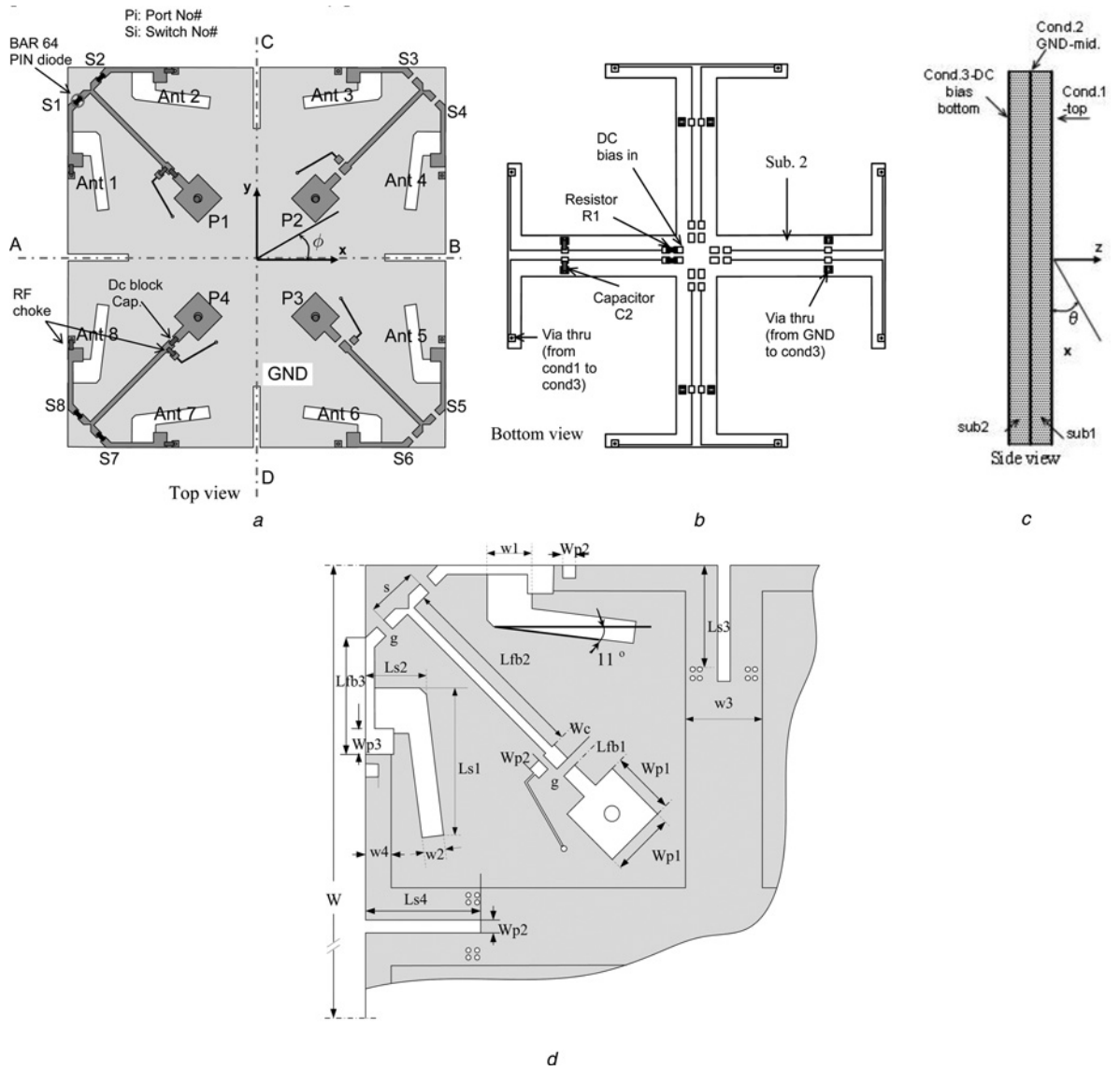

Fig. 1 *Proposed array antenna structure and notation*

a Top view
b Bottom view
c Side view
d Antenna dimension

Table 1 Detailed parameters of the proposed antenna array

Parameter	Value	Parameter	Value
ϵ_r	4.6	Lfb2	15.25
H	1.2	Lfb3	9
*R*1	100 Ω	Wp1	5
L1, L2	15 nH	Wp2	1
C1, C2	6.8 pF	Wp3	2
W	56	G	0.75
*w*1	3.5	Wc	1.5
*w*2	1.75	*L*s1	11.5
*w*3	6	*L*s2	4.75
Lfb1	2.63	*L*s3	7.85
s	4	*L*s4	9
R_f	3500 Ω	L_p	0.6 nH
R_r	0.85 Ω	C_r	0.23 pF

Length unit: mm

In this configuration of slot antenna, we create an L-shaped slot that represents a radiating element with 11° rotation compared with the ground edge as shown in Fig. 1*c*. This angle slot enhances the utilisation of the ground and beam shaping for the proposed antenna design. Moreover, four slits are added between the four-port antenna elements to increase the isolation between the near two ports. Both the 11°-angle slot and the slits reduce the mutual coupling effects while increasing the isolation between the two adjacent slots of the two adjacent ports. Each RF port has two switches to control the 'ON/OFF' states of its slots, making the slots act as magnetic dipoles. In the experimental antenna array, we select the BAR64 PIN diode for the active switches [17]. The combination of several states of suitable activated slots on the four RF-port outputs of the antenna array makes it multi-mode beam reconfigurable. The bias network for controlling the switches ON/OFF states is designed carefully to optimise the overall the antenna array performance.

doi: 10.1049/iet-map.2011.0606

2.2 Feed and switching bias network configuration

As each of the slots on the four-port array antenna can be selected by individually controlling the switch 'ON' or 'OFF' to orient an independently directive beam, a feed and switching network is required to activate or deactivate the slot that corresponds to the selection of the beams. Few options can be implemented as an active switch, such as MEMS, GaAs FET switches or PIN diodes. Each type of these active switches has it own advantages and disadvantages as discussed in [14]. In our proposed design, we select the Infineon BAR64-02V PIN diode as the switch in order to attain compact size, low cost, high isolation and minimum loss. Figs. 2*a* and *b* show the equivalent circuit model of the BAR64-02V PIN diode in the 'ON' and 'OFF' state [17]. The values of R_f, L_p, R_r, C_r are extracted from the datasheet and measurement, and are listed in Table 1. These data values are then used for the lumped components modelled in our simulation setups. Fig. 2*c* shows the equivalent circuit of the proposed DC biasing network for switches 'S1' and 'S2'; L1 and L2 act as RF chokes, and *C*1 is a DC-blocking capacitor. When a DC bias voltage of $V\text{cc} = 3$ V, the PIN diode is 'ON', and the RF signal can pass through from port 1 (*P*1) to the ground slot antenna with small insertion loss. When a reverse bias is applied at $V\text{cc} = 0$ V, the PIN diode is 'OFF' due to high isolation from *P*1 to the open-ended microstrip feed line. Fig. 2*d* shows the simulated and measured ON/OFF state characteristic of the proposed switch circuit controlling network. The measurement of S_{11} and S_{21} for the BAR64 was performed with an Agilent8510C network analyser using the de-embedded through-reflect-line (TRL) technique. It shows that in the ON state the insertion loss is ~0.7 dB, and in the OFF state the isolation is ~28 dB at the operating frequency of 2.7 GHz. The antenna array is fed by four standard 50-Ω-MCX connectors with a coaxial cable connected at the bottom ground of the antenna.

2.3 Theory of operation modes

In the proposed design, we can easily change the centre resonant frequency f_c by optimising the value of the parameters *w*1, *w*2, *Ls*1, *Ls*2. Fig. 3 shows the changes in f_c by adjusting the *w*1, *Ls*1, and *Ls*2 parameters for a single antenna element. The designed parameters of (*w*1, *w*2, *Ls*1, *Ls*2), listed in Table 1, are the optimised values that lead to the optimum performance of array at the frequency region of 2.6–2.8 GHz. The simulated current distribution surface of the active slot and its radiation are shown in the Fig. 4. As shown in Fig. 4*a*, the current distributions are dominant around the L-shaped ground slot at the resonant frequency. These currents can be simply decomposed into three parts, named as $\boldsymbol{I}_1, \boldsymbol{I}_2$ and $\boldsymbol{I}_3$. The direction of the currents $\boldsymbol{I}_1$ and $\boldsymbol{I}_3$ are opposite that can be canceled by each other in some parts of phase and magnitude, therefore the main contribution is the current $\boldsymbol{I}_2^*$. Where, the phase is $\boldsymbol{I}_2^* = \boldsymbol{I}_1 + \boldsymbol{I}_2 + \boldsymbol{I}_3$ and the magnitude is $\boldsymbol{I}_2^* = (I_3 - I_1) + I_2$. Accordingly, the radiation patterns are similar to those of small magnetic dipoles, which laid in the *xy*-plane with the direction follow by the current $\boldsymbol{I}_2^*$ and are mainly contributed by current $\boldsymbol{I}_2^*$. Where the phase is $\boldsymbol{I}_2^* = \boldsymbol{I}_1 + \boldsymbol{I}_2 + \boldsymbol{I}_3$ and the magnitude is $\boldsymbol{I}_2^* = (I_3 - I_1) + I_2$. Accordingly, the radiation patterns are similar to those of small magnetic dipoles, which laid in the *xy*-plane with the direction followed by the current $\boldsymbol{I}_2^*$ and are mainly

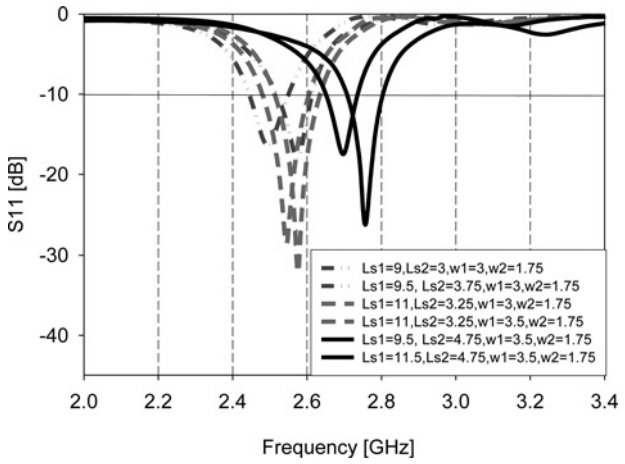

Fig. 3 *Simulated return loss for various structural configuration by adjusting slot parameters – unit length mm*

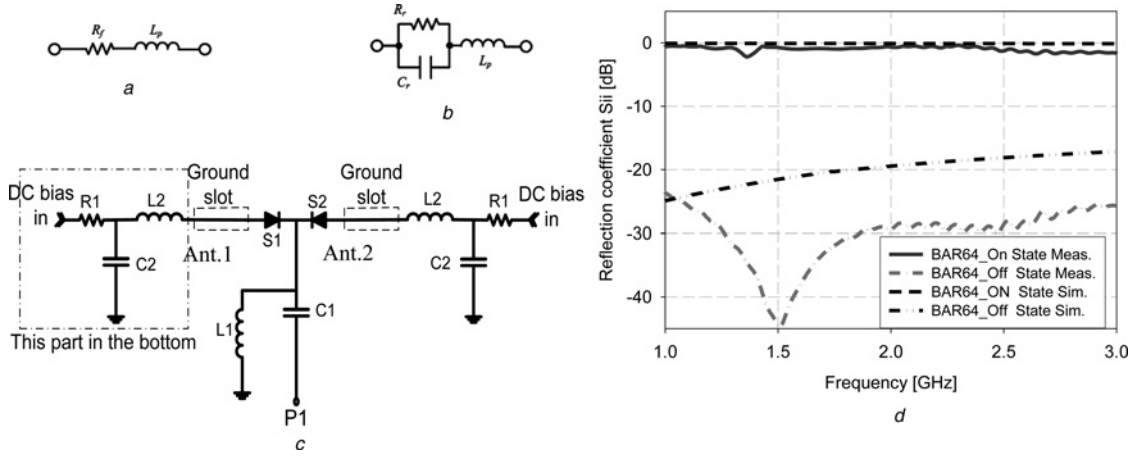

Fig. 2 *Proposed DC bias and switching circuit of BAR64 PIN diode and its characteristic in ON/OFF states*

a On state
b Off state
c Proposed DC bias and switching circuit for two switches of BAR64 PIN diodes
d Characteristic of BAR-64W02V PIN diode

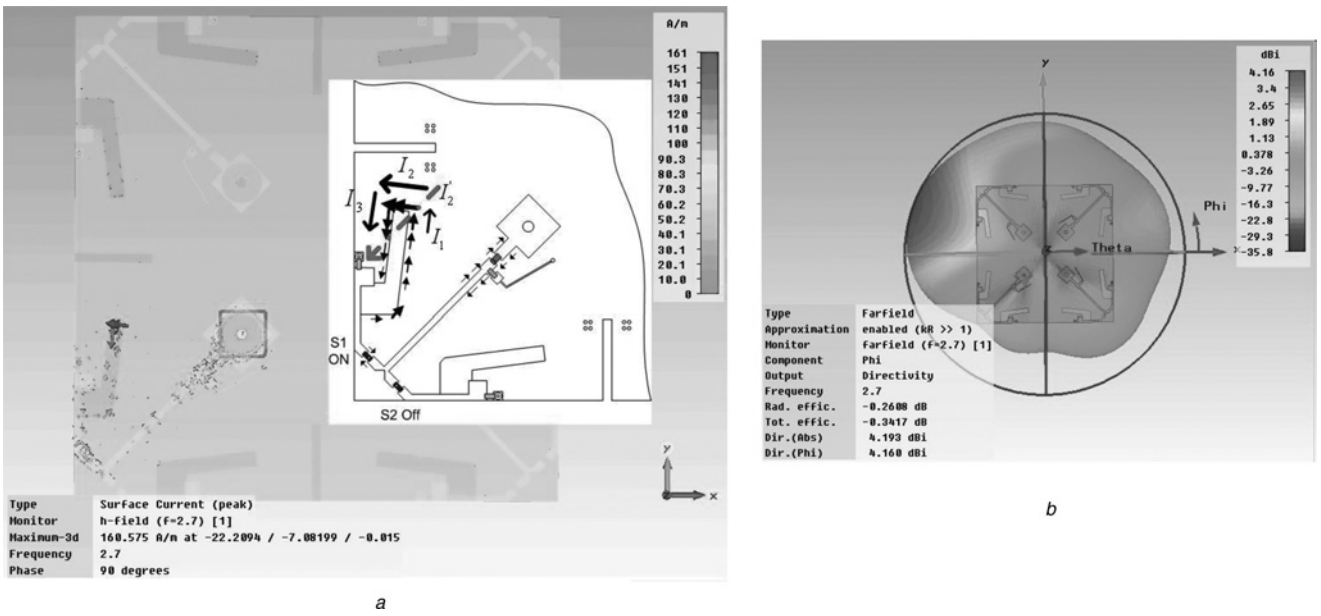

Fig. 4 *Simulated surface currents distribution and 3D beam pattern of one activated slot*

a Surface currents distribution of the activated slot
b 3D beam pattern

contributed by current I_2^*. This leads to the fact that the gain patterns G_ϕ in *xy*-plane and G_θ in the *yz*-plane are bidirectional, while G_ϕ in the *xz*-plane presents a nearly omni-directional radiation [5]. Furthermore, owing to the ground shape plane, G_ϕ in the *xy*-plane becomes directional, and the maximum radiation direction is outward from the open end of the slot of the adjacent port as shown in Fig. 4*b*. As discussed above, the L-shaped slot antenna presents a directional beam pattern in the azimuth plane. A directional beam pattern antenna is capable of alleviating multipath effects for a single-antenna system; however, it may cause problem when the desired signal comes from the directions of the nulls. As this compact planar slot antenna array has a symmetrical configuration, by subsequently changing the ON/OFF state of each slot we reach 360° coverage in the azimuth plane with a wide variety of directive beams.

3 Experimental and simulated results

The commercial EM full-wave simulator CST2009 is used to simulate and optimise the antenna parameters [21]. To validate the performance of the proposed antenna array, a 2.6–2.8-GHz switched beam four-port antenna array for small smart antenna applications is designed and fabricated as shown in Fig. 5. In the simulation setup, we also included the lumped model for the PIN diode in our proposed antenna array. The reflection coefficients (S_{11}) were measured with an Agilent-HP E8357A network analyser, and the antenna array radiation patterns were measured with an anechoic chamber of size of 10 (L) × 5 (H) × 6 m (W) at Korean Advanced Institute of Science and Technology. In the previous section, we discussed the theory of the operation and the beam pattern of antenna array by changing the state of the ON/OFF of switches. The combination of several states of appropriate slots on the four-port antenna array makes the antenna act as a multi-mode beam reconfigurable antenna. These modes are described as follows.

3.1 Mode 1: single port – single switch ON

For example, switch 8 (Sw8) at port 4 (P4) is ON. The simulated and measured reflection coefficients and its radiation patterns are shown in Figs. 6*a* and *b*, respectively. Fig. 6*c* shows the measured beam patterns, which are rotated in the *xy*-plane with 360° coverage by sequently changing from Sw1 to Sw8 'ON' at a time from P1 to P4. In this mode, the bandwidth is about 130 MHz at the centre frequency of 2.75 GHz, and the measured gain pattern is ~3.2 dB.

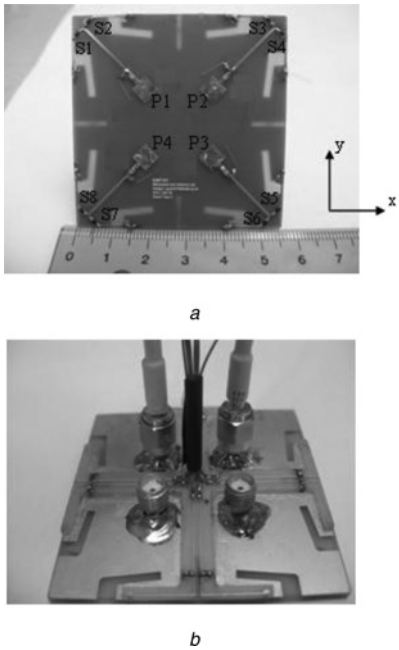

Fig. 5 *Photograph of the fabricated array antenna*

a Top view
b Bottom view

doi: 10.1049/iet-map.2011.0606

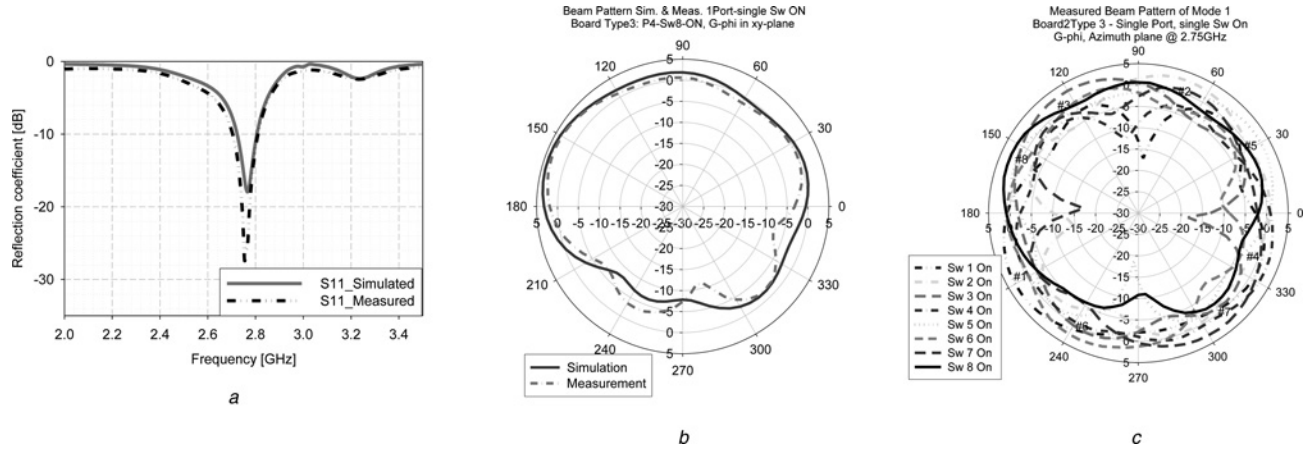

Fig. 6 *Simulated and measured reflection coefficients and its radiation patterns of P4Sw8 is ON*

a Simulated and measured reflection coefficients
b Its radiation patterns
c Sequential rotation beam patterns by changing each switch ON from P1 to P4

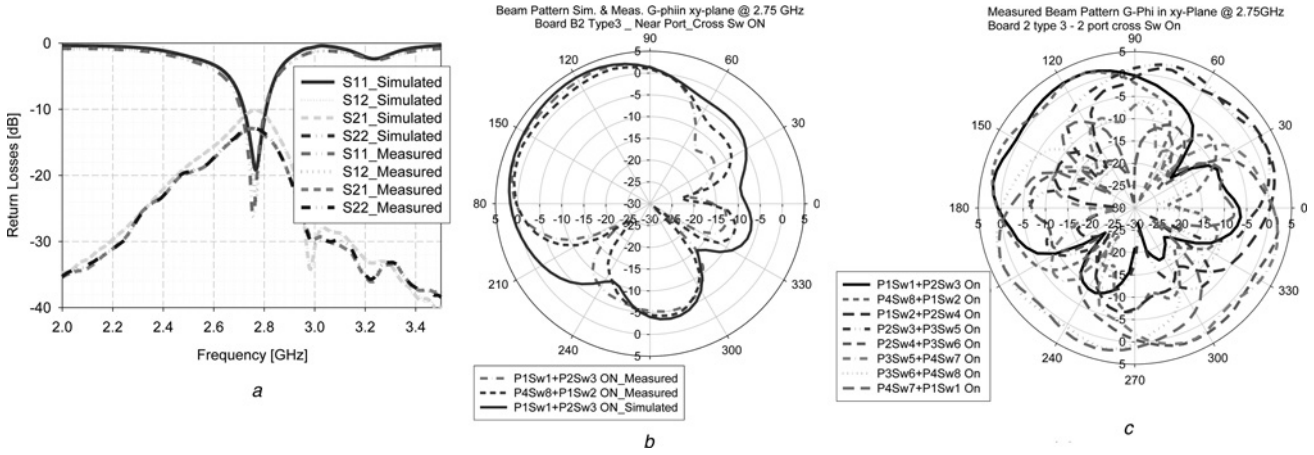

Fig. 7 *Simulated and measured reflection coefficients and its radiation patterns of P1Sw1 + P2Sw3 or P1Sw2 + P4Sw8 are ON*

a Simulated and measured reflection coefficients
b Its radiation patterns
c Reconfigurable beam patterns by sequently changing each switch ON at two ports (2 port cross Sw ON)

3.2 Mode 2: two ports – single, cross switch ON per port

For example, Sw1 on P1 and Sw3 on P2 are 'ON' (P1Sw1 + P2Sw3). The simulated and measured refection coefficients and isolations at two ports, and its radiation patterns are shown in Figs. 7*a* and *b*. Similarly, if we sequently change the ON switches from P1Sw1 + P2Sw3 to P1Sw2 + P2Sw4, the beam pattern rotates 90° in the *xy*-plane, as shown in Fig. 7*c*. For this mode, the bandwidth is ~100 MHz at 2.75 GHz, and the measured isolation at the two ports is ~ − 14 dB. The measured gain G_ϕ pattern is ~3 dB. The maximum radiation pattern direction is pointed to 45, 135, 225 and 315°.

3.3 Mode 3: near two port – opposite switch ON

For example, Sw2 on P1 and Sw7 on P4 are ON (P1Sw2 + P4Sw7). The resonance occurs at the centre frequency of ~2.75 GHz under the reflection coefficients of −10 dB. The measured bandwidth is ~110 MHz. The isolation between the two-port is approximately of −13 dB. In this mode the null of beam patterns is turned around 0–90–180 and 270°. The simulated and measured refection coefficients and their radiation patterns are shown in Fig. 8. The gain pattern G_ϕ in the azimuth plane is the maximum radiation direction to the angle of 45, 135, 225 and 315°. The measured beam patterns when we sequently change the state of switch on each port in clockwise of this mode are shown in Fig. 8*c*. The measured gain G_ϕ pattern is ~2.7 dB.

3.4 Mode 4: cross port – opposite switch ON

An example of this mode is Sw2 on P1 and Sw5 on P3 ON (P1Sw2 + P3Sw5). Fig. 9 shows the simulated and measured reflection coefficients and the radiation patterns of P1Sw2 + P3Sw5 ON. The measured beam patterns when we sequently change the state of switch on each port clockwise of this mode are shown in Fig. 9*c*. The bandwidth of this mode is ~150 MHz at 2.75 GHz and the isolation between the P1 and P4 is ~ − 13 dB for the measured results. It can be seen that the shape of beam patterns is similar to those of mode 4; however, in this mode it is rotated 45°. The maximum radiation direction is

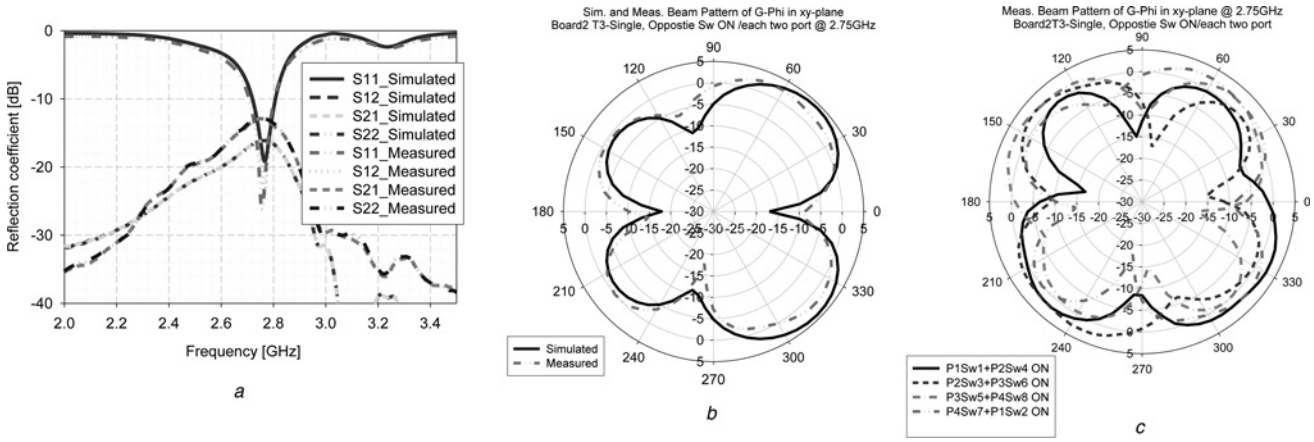

Fig. 8 *Simulated and measured reflection coefficients and its radiation patterns of P1Sw2 and P4Sw7 are ON*

a Simulated and measured reflection coefficients
b Its radiation patterns
c Reconfigurable beam patterns by sequently changing opposite switch ON in each port

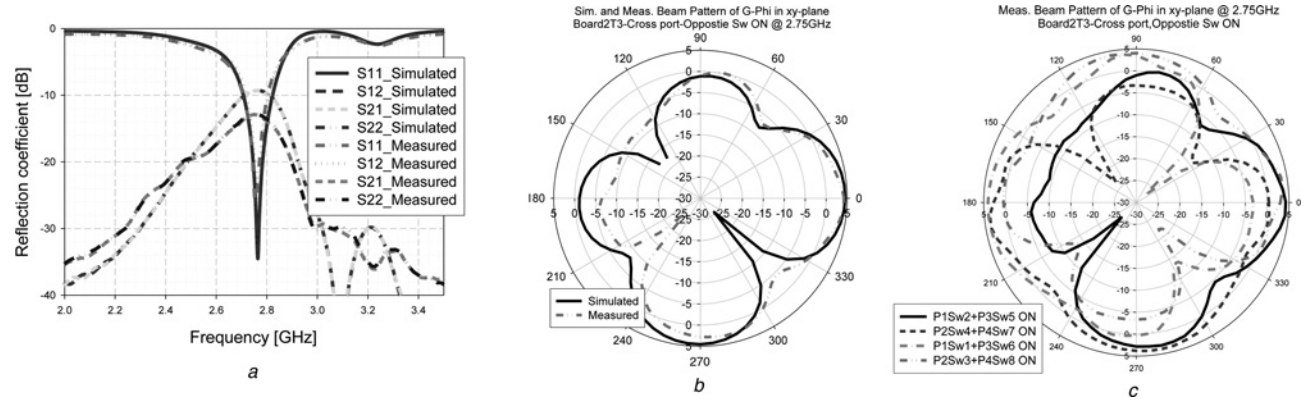

Fig. 9 *Simulated and measured reflection coefficients and its radiation patterns of P1Sw2 and P3Sw5 are ON*

a Simulated and measured reflection coefficients
b Its radiation patterns
c Rotation of the beam patterns by sequently changing opposite Sw ON at each cross two ports

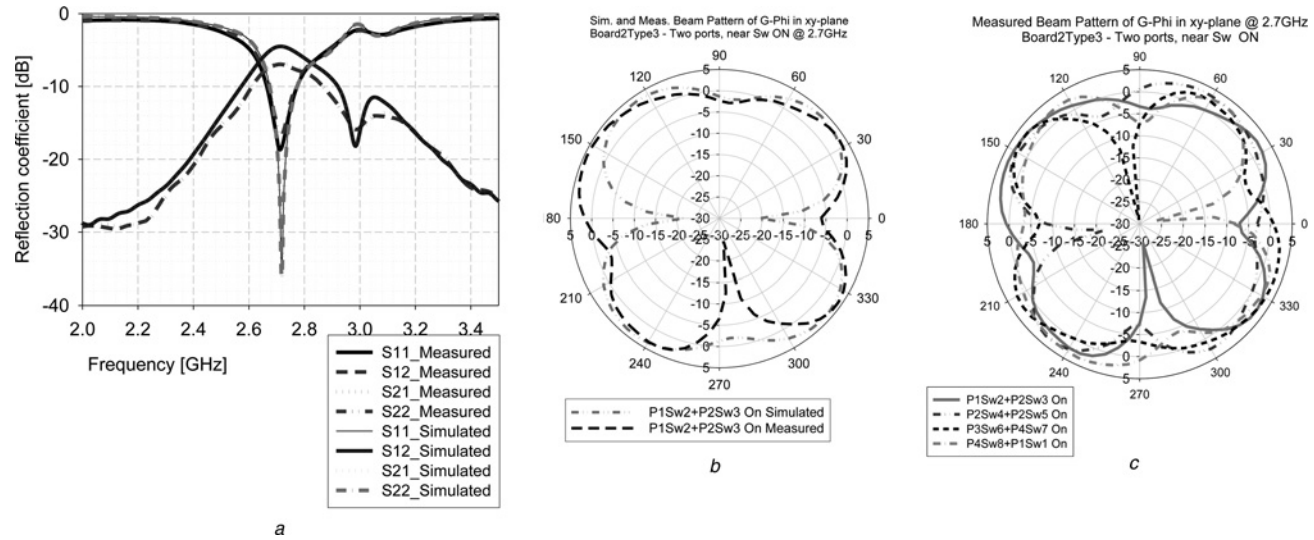

Fig. 10 *Simulated and measured reflection coefficients and its radiation patterns of P1Sw2 + P2Sw3 are ON*

a Simulated and measured reflection coefficients
b Its radiation patterns
c Rotation of the beam patterns by sequently changing each near switch ON in each port

doi: 10.1049/iet-map.2011.0606

pointed to 0–270°, and the null is 315°. The measured gain pattern is ~4 dB.

3.5 Mode 5: two ports-near sw ON per port

On mode 5, we verify the Sw2 at P1 and Sw3 at P2 are ON. The simulated and measured refection coefficients and radiation patterns are shown in Fig. 10. Similar to the operation in mode 3, owing to the coupling effects of closed ports and near activated ground slots, the measured centre frequency of the resonance is shifted down to 2.7 GHz, and the measured isolation between the two ports is ~7.5 dB. The bandwith is ~130 MHz. The measured beam patterns when we sequently change the state of switch on each port from P1 to P4 clockwise are shown in Fig. 10*c*.

4 Discussion

4.1 Calculated envelope correlations

Space diversity is a well-known technique for improving signal quality in a wireless communication system. In fact, diversity antenna gain is an important factor for the improvement of a diversity antenna system compared with a single-antenna system. Antenna system performance depends on the envelope correlations and power imbalance between the diverted signals [13]. A general form of envelope correlation can be calculated as [18]

$$\rho_e = \frac{\left|\iint_{4\pi} [\boldsymbol{F}_1(\theta, \phi) \bullet \boldsymbol{F}_2(\theta, \phi)]\, d\Omega\right|^2}{\iint_{4\pi} |\boldsymbol{F}_1(\theta, \phi)|^2\, d\Omega \iint_{4\pi} |\boldsymbol{F}_2(\theta, \phi)|^2\, d\Omega} \quad (1)$$

where $d\Omega = \sin\theta\, d\theta\, d\phi$, and $\boldsymbol{F}_1(\theta, \phi)$ is the radiated electric field of the ith operation mode. However, this formulation is quite complicated to calculate the envelope correlation coefficient. In [18], Grand used another expression that leads to a fast characterisation of the correlation and provides a better insight into the effects of mutual coupling by using the measurements of the S-parameters, which is less complex and takes less time than the measurements of the field patterns.

$$\rho_e = \frac{|S_{11}^* S_{12} + S_{21}^* S_{22}|^2}{(1 - (|S_{11}|^2 + |S_{21}|^2))(1 - (|S_{22}|^2 + |S_{12}|^2))} \quad (2)$$

It is shown that (2) of the envelope correlation using the S-parameters can be considered as a good approach [18]. Table 2 shows the simulated and measured envelope correlations between the operation modes of the designed antenna array. If the correlation is high, the received signals may suffer from deep fading simultaneously. According to [19, 20], the criteria $\rho_e < 0.5$ is necessary to obtain an obvious improvement from a diversity system.

Table 2 Envelope correlations between operation modes of the designed antenna array

Mode	ρ_e	
	Simulated	Measured
mode 2	0.2575	0.214
mode 3	0.197	0.1088
mode 4	0.261	0.208
mode 5	0.3872	0.411

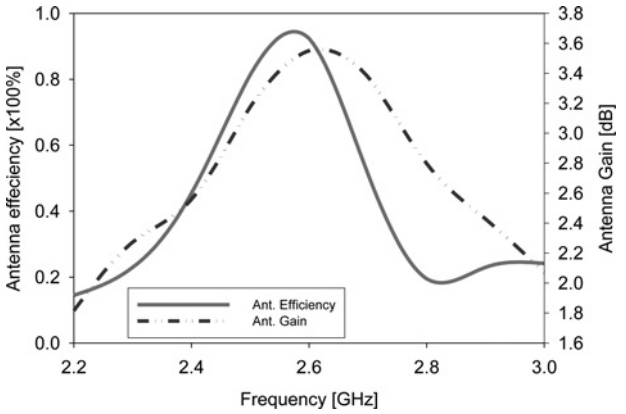

Fig. 11 *Simulated gain and efficiency characteristics of the antennas considering the losses caused by PIN diodes*

4.2 Advantages

The simulated and fabricated antenna shows that the reflection coefficients of the proposed antenna array for most operating modes are lower than −10 dB with sufficient bandwidth. This antenna design is also a cost-effective solution as it composes of a common cheap FR4 substrate and several lumped elements. Table 3 shows the comparison of this proposed antenna array with published planar reconfigurable beam antennas [5, 7]. Fig. 11 shows the simulated gain and efficiency characteristics of the antennas considering the losses caused by PIN diodes. The simulated radiation efficiency is 95% at the resonant frequency.

5 Conclusion

A compact, planar four-port switched and reconfigurable antenna array has been proposed. The integration of antenna elements, feed and bias switching networks has been considered. The proposed antenna has been built with an optimal and compact size that is appropriate for an array configuration in order to have a reconfigurable beam pattern. The antenna beam pattern characteristic is suitable

Table 3 Comparison between the proposed antenna array with the traditional reconfigurable beam antennas

Ref.	f_c, GHz	Sub.	Size in square	Measured gain, dBi	Measured BWMHz $S_{11} < -10$ dB	No. of directional beam
[5]	2.45	FR4, 4.4	$0.43\lambda_o$	−0.5 ~ 2.1	90	8+
[7]	2.45	roger 4003	$1.92\lambda_o$	6.7	100	6+
this work	2.7	FR4, 4.6	$0.5\lambda_o$	~4	130	20+

for smart antenna applications and MIMO systems. It covers 360° in the azimuth plane with the maximum at the direction beam up to ~4 dB. The antenna is able to control the beam pattern so as to be directed to the desired incoming signal. The experimental results fully demonstrate the performance of the fabricated antenna. There is good agreement between the simulation results and experimental results.

This switched beam planar antenna, which can be implemented as a compact and low-cost switched and reconfigurable beam antenna array without phase shifters, is a very promising approach for small smart antenna systems and MIMO systems. The experimentation and simulation results shows that the proposed antenna array performances are sufficiently good for beam selectivity systems.

6 References

1 Jiajie, Z., Anguo, W., Peng, W.: 'A survey on reconfigurable antennas'. Int. Conf. on Microwave and Millimeter Wave Technology-ICMMT, 2008, vol. 3, pp. 1156–1159

2 Cheng, W.H., Feng, Z.H.: 'Planar reconfigurable pattern antenna by reactive-load switching', *Microw. Opt. Technol. Lett*, 2005, **47**, (5), pp. 506–507

3 Piazza, D., Kirsch, N.J., Forenza, A., Heath, R.W., Dandekar, K.R.: 'Design and evaluation of a reconfigurable antenna array for MIMO systems', *IEEE Trans. Antennas Propag.*, 2008, **56**, pp. 869–881

4 Wu, S.-J., Ma, T.-G.: 'A wideband slotted bow-tie antenna with reconfigurable CPW-to-slotline transition for pattern diversity', *IEEE Trans. Antennas Propag.*, 2008, **56**, pp. 327–334

5 Lai, M.-I., Wu, T.-Y., Hsieh, J.-C., Wang, C.-H., Jeng, S.-K.: 'Compact switched-beam antenna employing a four-element slot antenna array for digital home applications', *IEEE Trans. Antennas Propag.*, 2008, **56**, pp. 2929–2936

6 Lai, M.-I., Jeng, S.-K.: 'Compact pattern reconfigurable antenna array based on *L*-shaped slots and PIN diodes for adaptive MIMO systems'. *IEEE Antennas Propag. Soc. Int. Symp.*, 2008, **8**, (1), pp. 6–9

7 Mark, A.C.K., Corbett, R.R., Ross, D.M.: 'Low cost reconfigurable landstorfer planar antenna array', *IEEE Trans. Antennas Propag.*, 2009, **57**, (10), p. 3051

8 Lai, M.-I., Wu, T.-Y., Hsieh, J.-C., Wang, C.-H., Jeng, S.-K.: 'A compact pattern reconfigurable antenna design for handheld wireless devices'. *IEEE Antennas Propag. Soc. Int. Symp.*, 2007, **1**, pp. 5223–5226

9 Peroulis, D., Sarabandi, K., Katehi, L.P.B.: 'Design of reconfigurable slot antennas', *IEEE Trans. Antennas Propag.*, 2005, **53**, pp. 645–654

10 Nair, S.V.S., Max, J.A.: 'Reconfigurable antenna with elevation and azimuth beam switching', *IEEE Antennnas Wirel. Propag. Lett.*, 2010, **9**, pp. 367–370

11 Piazza, D., Mookiah, P., D'Amico, M., Dandekar, K.R.: 'Experimental analysis of pattern and polarization reconfigurable circular patch antennas for MIMO systems', *IEEE Trans. Veh. Technol.*, 2010, **59**, pp. 2352–2362

12 Mak, A.C.K., Rowell, C.R., Murch, R.D., Mak, C.L.: 'Reconfigurable multiband antenna designs for wireless communication devices', *IEEE Trans. Antennas Propag.*, 2007, **55**, (7), pp. 1919–1928

13 Saunders, S.R.: 'Antenna and propagation for wireless communication system' (Wiley, New York, 1999)

14 Kraus, J.D., Marhefka, R.J.: 'Antennas for all applications' (McGraw-Hill, New York, 3rd edn.)

15 Gao, S.C., Li, L.W., Leong, M.S., Yeo, T.S.: 'Integrated multi-beam dual polarized planar array'. Proc. Int. Electrical Engineering Microwave Antennas Propagation, 2001, vol. 148, pp. 174–178

16 Mailloux, R.J.: 'Phased array antenna handbook' (Artech House Publishers, 2005, 2nd edn.)

17 Infineon datasheet of BAR64-02V.pdf Available at http://www.infineon.com/dgdl/bar64series.pdf

18 Dossche, S., Romeu, J., Blanch, S.: 'Representation of the envelope correlation as a function of distance and frequency for a two-port antenna system', *IEEE Antennas Propag. Soc. Int. Symp.*, 2004, **2**, pp. 1728–1731

19 Vaughan, R.G., Andersen, J.B.: 'Antenna diversity in mobile communications', *IEEE Trans. Veh. Technol.*, 1987, **VT-36**, pp. 149–172

20 Karaboikis, M., Soras, C., Tsachtsiris, G., Makios, V.: 'Compact dual-printed inverted-F antenna diversity systems for portable wireless devices', *IEEE Antennas Wirel. Propag. Lett.*, 2004, **3**, pp. 9–14

21 CST Microwave Studio 2009 by Computer Simulation Technology [Online]. Available at: http://www.cst.com

doi: 10.1049/iet-map.2011.0606